American Mineralogist, Volume 96, pages 74–80, 2011

Equation of state of carbonated hydroxylapatite at ambient temperature up to 10 GPa: Significance of carbonate

Xi Liu,[1,*] Sean R. Shieh,[2] Michael E. Fleet,[2] Lifei Zhang,[1] and Qiang He[1]

[1]The Key Laboratory of Orogenic Belts and Crustal Evolution, Ministry of Education of China, School of Earth and Space Sciences, Peking University, Beijing 100871, China
[2]Department of Earth Sciences, University of Western Ontario, London, Ontario N6A 5B7, Canada

Abstract

The incorporation of the carbonate ion into the crystal structure of hydroxylapatite results in the creation of vacancies, oxygen-loss, and disorder, with consequent changes in physical and chemical properties. High-pressure experimental investigation up to 10 GPa of two synthetic carbonated hydroxylapatite samples with up to 11 wt% CO_3, using a diamond-anvil cell and synchrotron powder X-ray diffraction, provides the first rigorous assessment of the mechanical behavior of the carbonated hydroxylapatite. The pressure-volume data suggest that the isothermal bulk modulus of these carbonated hydroxylapatites has been significantly decreased by the presence of the carbonate (up to about 15%), which in turn will affect all the carbonated apatite-related reactions in the geosystem. Since hydroxylapatite is one of the major components of the bones and teeth, the incorporation of the carbonate in the hydroxylapatite weakens teeth and bones not only chemically, but also physically.

Keywords: Carbonated hydroxylapatite, isothermal bulk modulus, equation of state, synchrotron X-ray diffraction

Introduction

Apatite commonly occurs in sedimentary, igneous, and metamorphic rocks (e.g., Walters and Luth 1969; McClellan 1980; Lang et al. 1995; Santos and Clayton 1995; Comodi and Liu 2000), and it has been regarded as the tenth most abundant mineral on the Earth (McClellan and Lehr 1969; Hughes and Rakovan 2002). In most geological settings, it is present as an accessory phase, but in some other cases it can appear as a major phase; for example, its proportion in the pyroxenite of the Triassic-Jurassic silica-undersaturated alkalic intrusions in the Cordillera of British Columiba is about 10% (Lang et al. 1995). Due to its ubiquitous geological presence and crystal-structure chemical characteristics, such as extensive anion/cation substitution and volatile content (Hughes and Rakovan 2002; Pan and Fleet 2002), apatite has numerous useful geological applications, especially in dating and petrogenesis (e.g., Li et al. 2000; Filiberto and Treiman 2009).

The general chemical formula of apatite can be written as $A_{10}(BO_4)_6X_2$, where A = Na^+, Ag^+, Ca^{2+}, Pb^{2+}, and rare-earth elements (REE^{3+}), B = P^{5+}, C^{3+}, S^{6+}, Si^{4+}, As^{5+}, and V^{5+}, and X = F^-, $(OH)^-$, Cl^-, $(CO_3)^{2-}$, $(HCO_3)^-$, O^{2-}, neutral molecules like H_2O, and vacancies (Pan and Fleet 2002; Fleet and Liu 2007a). The geologically important species of apatite are fluorapatite [ideal formula $Ca_{10}(PO_4)_6F_2$], hydroxylapatite [ideal formula $Ca_{10}(PO_4)_6(OH)_2$], chlorapatite [ideal formula $Ca_{10}(PO_4)_6Cl_2$], and carbonated apatite with variable formula. The structural details of fluorapatite, hydroxylapatite, and chlorapatite have been generally well established (e.g., Hughes et al. 1989) while those of carbonated apatite have not been fully disclosed, as outlined below. It has been experimentally shown that apatite can be stable up to the *P-T* conditions of the upper mantle of the Earth [about 12 GPa; Murayama et al. (1986)], so that the equation of state of apatite could be very important. So far, compression experiments have been carried out to investigate the compressibility of fluorapatite, hydroxylapatite, and chlorapatite (Brunet et al. 1999; Comodi et al. 2001; Matsukage et al. 2004), but no comparable work has been done on the carbonated apatite. Additional closely-related experimental studies include Liu et al. (2008) [lead fluorapatite $Pb_{10}(PO_4)_6F_2$] and Fleet et al. (2010) (lead fluorapatite), and Zhai et al. (2009) [γ-tricalcium phosphate γ-$Ca_3(PO_4)_2$, the main breakdown product of apatite].

As mentioned above, the formula of carbonated apatite is highly variable, and this is mainly because carbonate can substitute for both the channel anion and the phosphate ion: the former carbonate is referred to as type A while the latter is type B (e.g., LeGeros 1965; Trueman 1966; LeGeros et al. 1969; Elliott et al. 1980; Regnier et al. 1994; Nathan 1996). Due to the importance of the carbonated hydroxylapatite in biomineralization (Elliott 1994, 2002), the incorporation of carbonate in apatite and its resulting physical-chemical changes have been actively explored and intensely debated (e.g., Wilson et al. 1999; Leventouri et al. 2000, 2001; Fleet and Liu 2003, 2004, 2005, 2007b, 2008a, 2008b, 2009; Fleet et al. 2004; Wilson et al. 2004; Fleet 2009). In particular, it has been shown that the incorporation of carbonate into the structure of apatite can enhance the solubility of apatite (LeGeros 1991). Here we investigate the effect of the carbonate ion on the compressibility of the apatite.

Experimental methods

The materials used in the high-pressure experiments reported here were samples LM006 {$[Ca_{9.66}Na_{0.35}][(PO_4)_{5.56}(CO_3)_{0.44}][(OH)_{1.45}(CO_3)_{0.33}]$; 4.8 wt% CO_3} and LM005 {$[Ca_{9.13}Na_{0.87}][(PO_4)_{5.05}(CO_3)_{0.95}][(OH)_{0.36}(CO_3)_{0.86}]$; 11.2 wt% CO_3} (Fleet and Liu 2007b). These two samples have been characterized previously by

* E-mail: xi.liu@pku.edu.cn

several analytical methods such as electron probe microanalysis, FTIR spectroscopy, powder X-ray diffraction, and single-crystal X-ray diffraction, so that their compositional and structural details are well known. In particular, the occupancies of type A and type B carbonate were obtained by single-crystal X-ray structure refinement in Fleet and Liu (2007b). In LM005, the channel ion OH was almost completely replaced by the carbonate ion (~80%), so that LM005 can be generally treated as an end-member for the type-A carbonate apatite species. The IR spectra of the carbonated apatites change dramatically with the introduction of sodium (Fleet and Liu 2007b, 2008a, 2008b, 2009). In addition, these authors demonstrated that the synthetic sample LM006 is actually similar in both composition and IR spectrum to bovine bone and human dental enamel.

In-situ high-pressure angle dispersive X-ray powder diffraction experiments using a symmetrical diamond-anvil cell were carried out at beamline X17C, National Synchrotron Light Source, Brookhaven National Laboratory. T301 stainless steel plates were used as the gaskets, whereas a 4:1 methanol-ethanol mixture was used as the pressure medium. To determine the experimental pressure by the ruby fluorescence method (Mao et al. 1978), a couple of tiny ruby balls were loaded with the sample. The experimental techniques used here were almost identical to those reported in Liu et al. (2008), with the only exceptions that an online CCD detector rather than an image plate was used to collect the X-ray diffraction patterns and longer data-collecting times (20 min) were used. The hexagonal unit-cell parameters of the carbonated hydroxylapatites at different pressures were calculated by refining the unit cells using the diffraction peaks 200, 111, 002, 102, 210, 211, 112, 300, 202, 301, 212, 310, 311, 113, 203, 222, 312, 123, 321, 410, 402, and 004, whose positions were determined by full spectrum refinement of powder X-ray patterns. The present study was limited to powder diffraction measurements due to the fragility of the single-crystal products quenched from high pressure in Fleet and Liu (2007b).

Result and discussion

Hydrostatic high-pressure experiments were conducted up to about 10 GPa. No phase transition was observed for LM006 and LM005 over this pressure interval. Typical powder X-ray diffraction patterns for the carbonated hydroxylapatites are illustrated in Figure 1. The unit-cell parameters at different pressures derived from the X-ray diffraction patterns are listed in Table 1 and graphed in Figure 2.

Effects of carbonate on the cell parameter and elastic anisotropy of apatite

As reviewed in Fleet et al. (2004), the response of the unit-cell parameters of apatite to accommodation of the carbonate ion is complex. Substitution of hydroxyl (OH) by type A carbonate results in progressive increase in *a* and decrease in *c* (LeGeros et al. 1969; Bonel 1972), whereas substitution of phosphate by type B carbonate results in progressive decrease in *a* and increase in *c* (Nelson and Featherstone 1982; Vignoles et al. 1988). Thus, *a* and *c* were 9.557(3) and 6.872(2) Å for a synthetic end-member type A carbonate, $Ca_{10}(PO_4)_6CO_3$, (Elliott et al. 1980) and 9.437(1) and 6.888(1) Å, respectively, for a synthetic type B carbonate with one PO_4 group per formula unit replaced by CO_3 (Ivanova et al. 2001). The unit-cell parameters for the carbonate apatites quenched from high pressure in Fleet et al. (2004) and Fleet and Liu (2004, 2007b) were fully consistent with these earlier literature values. Additionally, the room-pressure data in Table 1 suggest that the *a*/*c* ratio was reduced by about 8‰ while the volume reduced by about 3‰ as the carbonate content increases from 0 to about 11.1 wt%, seemingly indicating only a minor effect of the carbonate.

High pressure reduces the size of the unit cell of the carbonated hydroxylapatites (Fig. 2). For the investigated pressure interval, the reduction of the lattice parameters *a* and *c* with pressure is slightly non-linear, and can be empirically described as: $a = 9.405(3) - 0.038(2)P + 0.0006(2)P^2$ and $c = 6.897(2) - 0.0017(1)P + 0.0002(1)P^2$ for sample LM006, and $a = 9.381(5) - 0.044(2)P + 0.0011(2)P^2$ and $c = 6.912(3) - 0.021(1)P + 0.0005(1)P^2$ for sample LM005, with *a* and *c* in angstroms and *P* in GPa (Fig. 2). In comparison, the dependence of *a* and *c* on pressure is linear for calcium fluorapatite but quadratic for lead fluorapatite

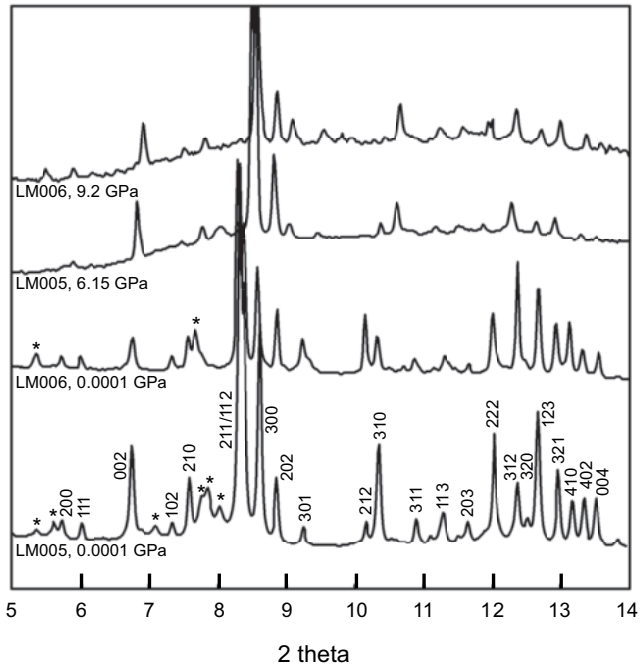

Figure 1. Examples of synchrotron X-ray diffraction patterns at 0.0001, 6.15 and 9.2 GPa. Note that a few weak peaks marked by the asterisks belong to an unidentified carbonate phase (Fleet and Liu 2007b). Room-pressure results were not collected in the diamond-anvil cell.

Table 1. Unit-cell parameters of carbonated hydroxylapatite at different pressures*

P (GPa)†	*a* (Å)	*c* (Å)	*V* (Å³)
	LM006		
0.0001	9.411(1)‡	6.900(1)	529.2(1)
1.1(1)	9.355(1)	6.875(1)	521.1(1)
2.14(7)	9.326(1)	6.863(1)	516.9(1)
3.22(5)	9.292(1)	6.846(1)	511.9(1)
4.08(3)	9.261(1)	6.830(1)	507.3(1)
5.08(3)	9.227(1)	6.820(1)	502.8(1)
6.1(2)	9.198(1)	6.798(1)	498.1(1)
7.1(1)	9.164(2)	6.787(2)	493.6(2)
8.2(1)	9.131(1)	6.771(2)	489.0(2)
9.2(2)	9.106(1)	6.756(1)	485.2(1)
	LM005		
0.0001	9.387(1)	6.913(1)	527.5(1)
1.79(3)§	9.306(1)	6.878(2)	515.8(1)
2.86(6)	9.253(2)	6.847(2)	507.7(2)
3.74(0)	9.231(1)	6.843(1)	505.0(1)
4.50(3)	9.211(2)	6.827(3)	501.6(2)
5.30(5)	9.178(2)	6.815(2)	497.1(2)
6.20(5)	9.154(1)	6.803(2)	493.6(1)
7.33(8)	9.123(2)	6.781(2)	488.8(2)
8.2(1)	9.096(1)	6.777(1)	485.4(1)
9.23(8)	9.072(1)	6.759(1)	481.7(1)
10.23(2)	9.041(1)	6.749(1)	477.7(1)

* All measurements at high pressures made in situ using a diamond-anvil cell.
† Pressure determined by averaging pressure values measured before and after collection of synchrotron data.
‡ Numbers in parentheses represent one standard deviation.
§ Data collected during decompression.

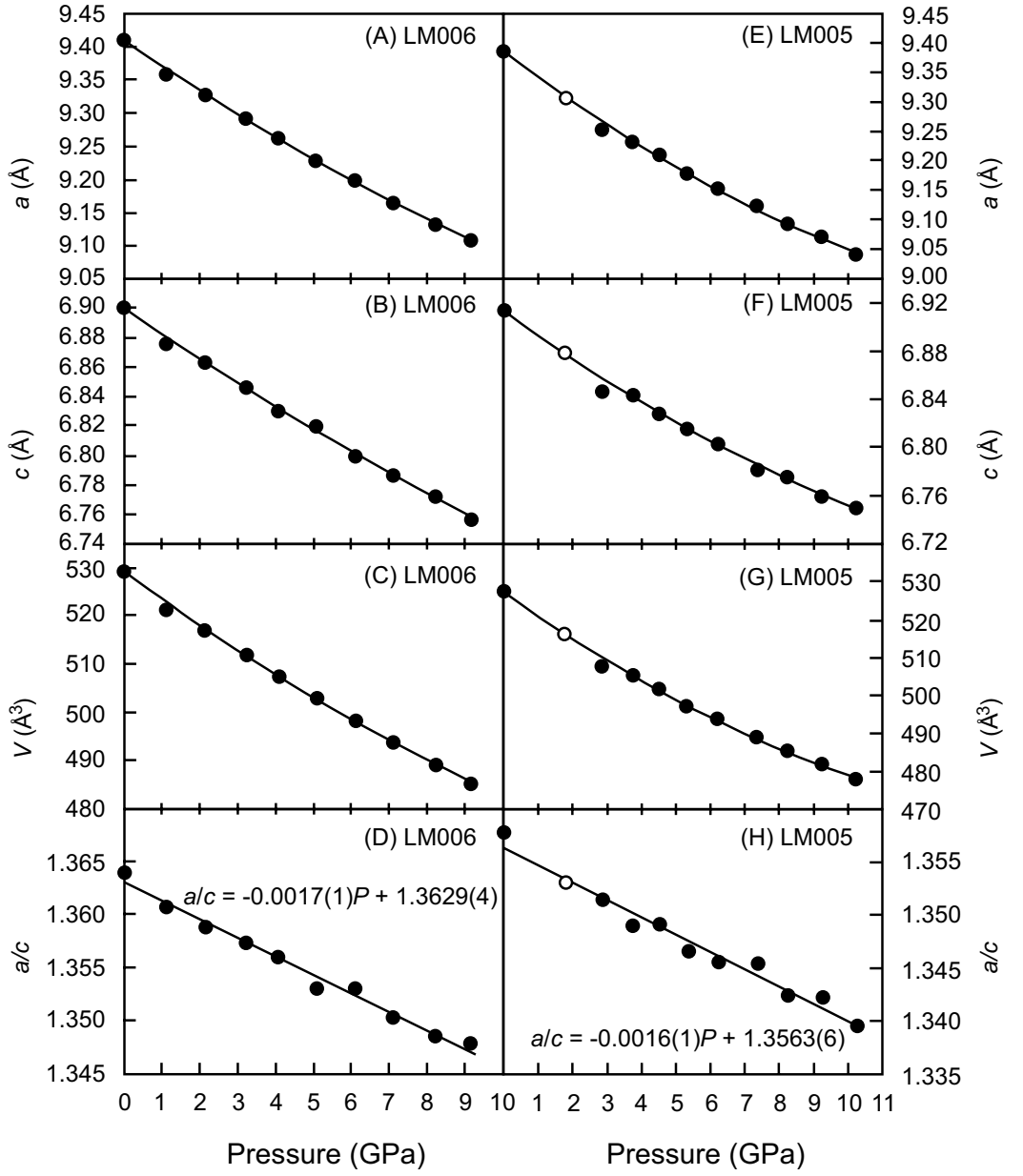

FIGURE 2. Variations in lattice parameters with change in pressure: A, B, C, and D are for LM006, whereas E, F, G, and H are for LM005. Filled symbols at pressures higher than room pressure stand for data collected during compression, whereas empty ones stand for data collected during decompression. Solid curves in A, B, C, E, F, and G represent the fitted axial and volume third-order Birch-Murnaghan equations of state (see text for more discussion). Note that all error bars are smaller than the symbol sizes.

(Comodi et al. 2001; Matsukage et al. 2004; Liu et al. 2008; Fleet et al. 2010). Similarly, the dependence of the volume on pressure can be empirically fitted as: $V = 528.4(5) - 5.5(2)P + 0.09(3)P^2$ for LM006, whereas $V = 526.8(7) - 6.5(3)P + 0.17(3)P^2$ for LM005. The *a*/*c* ratios of both LM006 and LM005 are negatively correlated with pressure, clearly indicating a reduction of the elastic anisotropy by pressure (Figs. 2d and 2h). The almost identical slopes of –0.0017(1) for LM006 and –0.0016(1) for LM005 (Figs. 2d and 2h) suggest that the incorporation of carbonate into the structure of hydroxylapatite does not result in any significant change in the effect of pressure on the elastic anisotropy of the apatites.

Effect of carbonate on the isothermal bulk modulus and its geological significance

To determine the isothermal bulk modulus, the *P*-*V* data of the carbonated hydroxylapatites have been fitted to the third-order Birch-Murnaghan equation of state (Birch 1947) by a least-squares method

$$P = 3K_T f_E(1 + 2f_E)^{5/2}[1 + 3/2(K_T' - 4)f_E]$$

where P is the pressure, K_T the isothermal bulk modulus, K_T' the first pressure derivative of K_T, and f_E the Eulerian definition of finite strain, which is $[(V_0/V)^{2/3} - 1]/2$, respectively. In the Eul-

erian definition of finite strain, V_0 is the volume at zero pressure, whereas V is the volume at high pressure. When K_T' is set as 4, the isothermal bulk modulus (K_T) of LM006 is 89.3(5) GPa and the zero-pressure volume is 529.16(8) Å^3. If K_T' is not fixed, the results of our best data-fitting for LM006 are K_T = 89(2) GPa, K_T' = 4.1(6), and V_0 = 529.17(9) Å^3. In contrast, when K_T' is set as 4, the isothermal bulk modulus (K_T) of LM005 is 84(1) GPa and the zero-pressure volume is 527.1(4) Å^3. If K_T' is not fixed, the results of our best data-fitting for LM005 are K_T = 73(2) GPa, K_T' = 7.0(6), and V_0 = 527.5(2) Å^3.

The quality of the derived third-order Birch-Murnaghan equation of state for the carbonated apatites can be evaluated by using the f_E-F plot (Fig. 3); F is defined as $F \equiv P/[3f_E(1 + 2f_E)^{5/2}]$. Using F, the third-order Birch-Murnaghan equation of state can be rewritten as:

$$F = K_T + 3/2K_T(K_T' - 4)f_E$$

so that the slope of the line defined by the experimental data should be equal to $3/2K_T(K_T' - 4)$, and the intercept value is the isothermal bulk modulus. Accordingly, a slope of zero means K_T' = 4, a negative slope $K_T' < 4$, and a positive slope $K_T' > 4$. Figure 3 clearly suggests that the K_T' of LM006 is close to 4 and the K_T' of LM005 is larger than 4, in agreement with our P-V data-fitting results detailed in the previous paragraph.

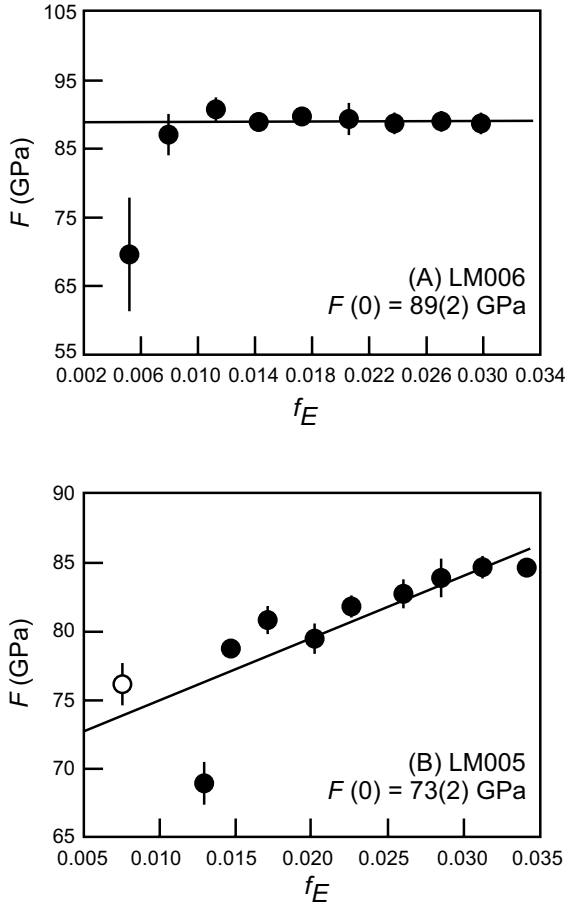

FIGURE 3. Volume Eulerian strain-normalized pressure (f_E-F) plots based on the Birch-Murnaghan equations of state: A is for LM006, whereas B is for LM005. Filled symbols at pressures higher than room pressure stand for data collected during compression, whereas empty ones stand for data collected during decompression. Estimated standard deviations have been calculated following the method in Heinz and Jeanloz (1984). The solid lines are the weighted linear fit through the data.

The isothermal bulk moduli of the carbonated hydroxylapatites are compared with those of other types of apatites in Figure 4. Also included here is a correlation analysis of K_T and K_T' for the carbonated hydroxylapatites obtained at fixed values of K_T'. To see the real difference that carbonate can make, only those studies with similar experimental techniques (here synchrotron X-ray radiation and high-pressure experimentation with diamond-anvil cell) have been used; other investigating techniques (both experimental and theoretical) tend to result in slightly different values for the bulk modulus of apatite (Gilmore and Katz 1982; Snyders et al. 2007; Ching et al. 2009). Compared to the isothermal bulk modulus of calcium hydroxylapatite [97.5 GPa from Brunet et al. (1999) when K_T' is set as 4], the isothermal bulk modulus of LM006 is about 10% smaller while that of LM005 is about 15% smaller. In contrast, previous compression experiments suggested that complete substitution of the volatile components F, Cl, and OH in the apatite channel has little influence on the isothermal bulk modulus (Brunet et al. 1999); this influence is generally smaller than, or at most identical to, the experimental uncertainty in the high-P compression experiments (Fig. 4). When Ca is replaced by Pb, on the other hand, the isothermal bulk modulus is reduced to only two-thirds of that of the calcium apatite (Liu et al. 2008).

A linearized third-order Birch-Murnaghan equation of state (Angel 2001) was used to obtain the parameters of the equations of state for the crystallographic axes, yielding: in the case of LM006, a_0 = 9.4105(9) Å, $K_{T\text{-}a}$ = 77(2) GPa, and $K_{T\text{-}a}'$ = 3.6(0.7) for the a-axis while c_0 = 6.8996(1) Å, $K_{T\text{-}c}$ = 130(5)

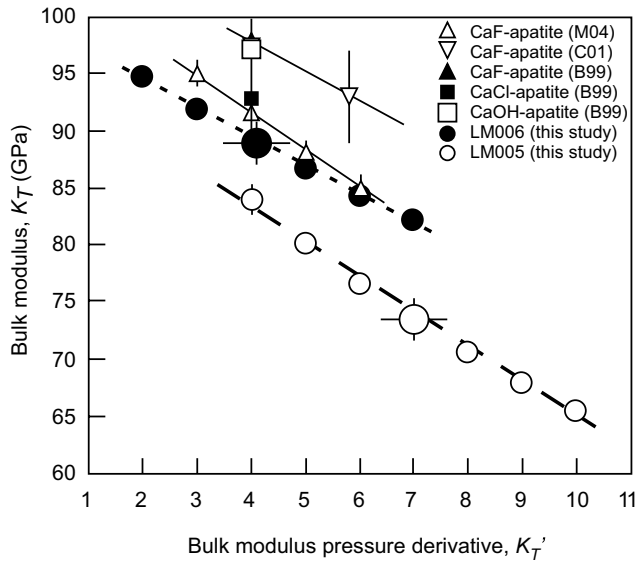

FIGURE 4. Comparison of the isothermal bulk moduli of carbonated hydroxylapatite with calcium hydroxylapatite–fluorapatite–chlorapatite [(CaOH-apatite)–(CaF-apatite)–(CaCl-apatite)] at ambient temperature. Large circles represent our best data-fitting results. B99 refers to Brunet et al. (1999), C01 Comodi et al. (2001) and M04 Matsukage et al. (2004).

GPa, and K'_{T-c} = 4(2) for the *c*-axis; in the case of LM005, a_0 = 9.387(2) Å, K_{T-a} = 64(2) GPa, and K'_{T-a} = 6.5(6) for the *a*-axis while c_0 = 6.913(2) Å, K_{T-c} = 104(7) GPa, and K'_{T-c} = 9(2) for the *c*-axis. The elastic anisotropy (K_{T-c}:K_{T-a}) of LM006 and LM005, therefore, is about 1.69 and 1.63, respectively; in other words, our two samples of carbonated hydroxylapatites show almost identical elastic anisotropy, with the *c*-axis direction is much less compressible than the *a*-axis direction. The quality of the derived third-order Birch-Murnaghan equation of state for the axes of the carbonated hydroxylapatites has been evaluated by using the f_E-F plot (Fig. 5).

The volume and axial isothermal bulk moduli of the carbonated hydroxylapatites are compared with those of the fluorapatite in Figure 6; currently there are no available experimental data, which can be used to derive the axial isothermal bulk modulus of hydroxylapatite. Apparently, the incorporation of carbonate ion into the structure has a very significant effect on the elastic properties: with the fluorapatite as a reference, the isothermal bulk moduli of LM005 have been reduced by more than 20% (Fig. 6a); there was evidence that the isothermal bulk moduli of fluorapatite and hydroxylapatite are almost identical (Brunet et al. 1999). Corresponding reduction in the axial isothermal bulk moduli has been observed as well (Figs. 6b and 6c).

Previous experiments suggested that fluorapatite and hydroxylapatite are stable up to the *P*-*T* conditions of the upper mantle (about 12 GPa; Murayama et al. 1986). Further thermodynamic analysis indicated that the stability of apatite might be somewhat reduced by the presence of silicate minerals such as kyanite and coesite/stishovite (Brunet et al. 1999). Despite the geological importance of apatite, how it breaks down at high pressures and what phases the breaking down reaction produces are largely unknown. What is certain from this investigation is that the breaking-down *P*-*T* curve should be significantly influenced by the incorporation of carbonate into the structure of apatite, as illustrated by the very different bulk moduli of the carbonate-free and carbonate-bearing apatites. Any exact thermodynamic evaluation of this effect, however, is currently hampered by the uncertainty identifying the breakdown product of apatite at high pressures.

Biological implication

Carbonated hydroxylapatite has been regarded as one of the major components of bones and teeth (bioapatite): it makes up about 73 wt% of cortical bone (which accounts for about 80% of the weight of the adult human skeleton), 96 wt% of dental enamel, and 73 wt% of dentine (Elliott 2002; Gross and Berndt 2002). Other components in bones and teeth include a small amount of water, and protein (mainly type I collagen) that

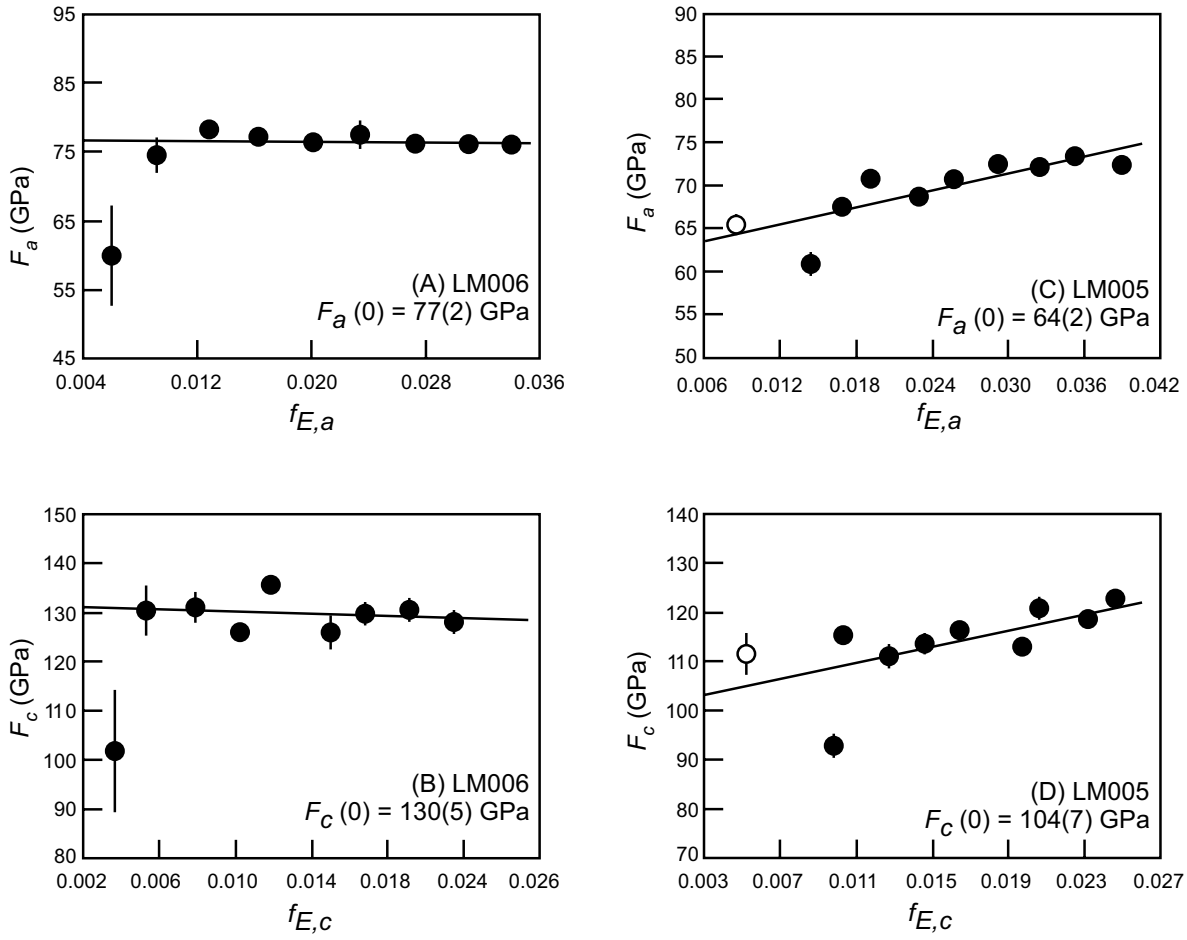

FIGURE 5. Axial Eulerian strain-normalized pressure (f_E-F) plots based on the Birch-Murnaghan equations of state: A and B are for LM006, whereas C and D are for LM005; see Figure 3 caption for further details.

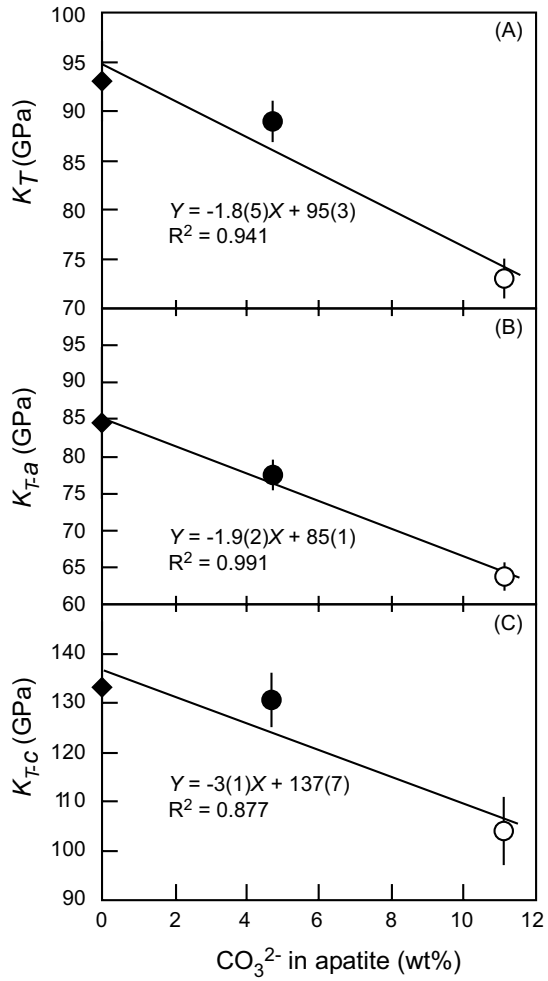

FIGURE 6. Effect of the carbonate content on the isothermal bulk modulus (K_T) of apatites at ambient conditions with any potential effect of sodium ignored. The filled diamond represents calcium fluorapatite, the filled circle LM006 and the empty circle LM005, respectively. The bulk modulus of the carbonate-free apatite is for calcium fluorapatite (Comodi et al. 2001).

holds the inorganic crystals together. According to the simulating models of the mechanical properties of bones and teeth, the elastic features of the carbonated hydroxylapatite are very important to the biological functions of the bones and teeth (e.g., Akiva et al. 1998; Rho et al. 1998; Katz et al. 2007). As clearly pointed out by Ching et al. (2009), however, neither reliable nor complete measurements are available for the anisotropic stress-strain-strength properties of biologically derived apatite. Our investigation reported here therefore provides critical data for future modeling.

The marked reduction in the strength of the carbonated hydroxylapatites compared with the carbonate-free apatites (Fig. 6) is readily attributable to the cumulated effects of vacancies, loss of oxygen and structural disruption resulting from the introduction of the carbonate ion (Fleet and Liu 2007b, 2008a, 2008b, 2009; Fleet 2009). Bioapatite contains approximately equal amounts of type A and type B carbonate (Fleet and Liu 2007b). The substitution of the phosphate (PO_4^{3-}) group by the carbonate ion (CO_3^{2-}) results in the loss of one oxygen atom and requires a charge-balancing parallel substitution that, most commonly, involves substitution of a calcium cation by sodium or a vacancy: e.g., [Na + CO_3 = Ca + PO_4]. Substitution of two hydroxyl ions by the bulky carbonate ion in the apatite channel (type A carbonate) does not require charge balancing but does require significant local dilation of the channel wall. Moreover, both type A and type B carbonate ions are randomly distributed and disordered throughout the structure. In the hexagonal space group $P6_3/m$ structure there are 12 possible orientations for both of the type A and type B carbonate ions (Fleet and Liu 2007b).

This investigation shows that carbonate content significantly reduces the isothermal bulk modulus of hydroxylapatite. We conclude that fluctuation in the carbonate content must have a profound influence on the elastic properties of bioapatite. Thus, both the proportion and carbonate content of bioapatite nanocrystals have to be taken into account in interpreting mechanical behaviour of bones and teeth. It is well known that carbonate content and minor magnesium and sodium impurities make enamel more susceptible to dental caries (Elliott 2002; Gross and Berndt 2002) because of their preferential dissolution; i.e., carbonate impurity weakens teeth (and bones) chemically. Our study shows that it must also weaken bones and teeth physically, by markedly reducing their strength and hardness.

ACKNOWLEDGMENTS

We are thankful for access to the National Synchrotron Light Source at Brookhaven National Laboratory, where the diffraction experiments were performed. We thank J. Hu for her help with the synchrotron X-ray diffraction measurements. Comments from two anonymous reviewers significantly improved this manuscript. G. Shen is thanked for his editorial handling. This investigation was financially supported by the National Natural Science Foundation of China (Grants 40872033 and 40821002) and by the Natural Sciences and Engineering Research Council of Canada (S.R. Shieh and M.E. Fleet).

REFERENCES CITED

Akiva, U., Wagner, H.D., and Weiner, S. (1998) Modeling the three-dimensional elastic constants of parallel-fibred and lamellar bone. Journal of Materials Science, 33, 1497–1509.

Angel, R.J. (2001) Equation of state. In R.M. Hazen and R.T. Downs, Eds., High-temperature and high-pressure crystal chemistry, 41, p. 35–60. Reviews in Mineralogy and Geochemistry, Mineralogical Society of America, Chantilly, Virginia.

Birch, F. (1947) Finite elastic strain of cubic crystals. Physical Reviews, 71, 809–924.

Bonel, G. (1972) Contribution à l'étude de la carbonatation des apatites. I. Synthèse et étude des propriétés physico-chimiques des apatites carbonatées du type A. Annales de Chimie (Paris, France), 7, 65–88.

Brunet, F., Allan, D.R., Redfern, S.A.T., Angel, R.J., Miletich, R., Reichmann, H.J., Sergent, J., and Hanfland, M. (1999) Compressibility and thermal expansivity of synthetic apatites, $Ca_5(PO_4)_3X$ with X = OH, F and Cl. European Journal of Mineralogy, 11, 1023–1035.

Ching, W.Y., Rulis, P., and Misra, A. (2009) Ab initio elastic properties and tensile strength of crystalline hydroxyapatite. Acta Biomaterialia, 5, 3067–3075.

Comodi, P. and Liu, Y. (2000) CO_3 substitution in apatite: Further insight from new crystal-chemical data of Kasekere (Uganda) apatite. European Journal of Mineralogy, 12, 965–974.

Comodi, P., Liu, Y., Zanazzi, P.F., and Montagnoli, M. (2001) Structural and vibrational behaviour of fluorapatite with pressure. Part I: In situ single-crystal X-ray diffraction investigation. Physics and Chemistry of Minerals, 28, 219–224.

Elliott, J.C. (1994) Structure and chemistry of the apatites and other calcium orthophosphates. Elsevier, Amsterdam.

——— (2002) Calcium phosphates biominerals. In M.J. Kohn, J. Rakovan, and J.M. Hughes, Eds., Phosphates: Geochemical, geobiological, and materials importance, 48, p. 427–453. Reviews in Mineralogy and Geochemistry, Mineralogical Society of America, Chantilly, Virginia.

Elliott, J.C., Bonel, G., and Trombe, J.C. (1980) Space Group and lattice constants of $Ca_{10}(PO_4)_6CO_3$. Journal of Applied Crystallography, 13, 618–621.

Filiberto, J. and Treiman, A.H. (2009) Martian magmas contained abundant chlorine, but little water. Geology, 37, 1087–1090.

Fleet, M.E. (2009) Infrared spectra of carbonate apatites: ν_2-Region bands. Bio-

materials, 30, 1473–1481.
Fleet, M.E. and Liu, X. (2003) Carbonate apatite type A synthesized at high pressure: new space group ($P\bar{3}$) and orientation of channel carbonate ion. Journal of Solid State Chemistry, 174, 412–417.
——— (2004) Location of type B carbonate ion in type A-B carbonate apatite synthesized at high pressure. Journal of Solid State Chemistry, 177, 3174–3182.
——— (2005) Local structure of channel ions in carbonate apatite. Biomaterials, 26, 7548–7554.
——— (2007a) Hydrogen-carbonate ion in synthetic high-pressure apatite. American Mineralogist, 92, 1764–1767.
——— (2007b) Coupled substitution of type A and B carbonate in sodium-bearing apatite. Biomaterials, 28, 916–926.
——— (2008a) Accommodation of the carbonate ion in fluorapatite synthesized at high pressure. American Mineralogist, 93, 1460–1469.
——— (2008b) Type A-B carbonate chlorapatite synthesized at high pressure. Journal of Solid State Chemistry, 181, 2494–2500.
——— (2009) Location of carbonate ions in structure of biological apatite. In R. Narayan and P. Colombo, Eds., Advances in Bioceramics and Porous Ceramics, 29, p. 63–76. Ceramic Engineering and Science Proceedings, Wiley, New York.
Fleet, M.E., Liu, X., and King, P.L. (2004) Accommodation of the carbonate ion in apatite: An FTIR and X-ray structure study of crystals synthesized at 2–4 GPa. American Mineralogist, 89, 1422–1432.
Fleet, M.E., Liu, X., and Shieh, S.R. (2010) Structural change in lead fluorapatite at high pressure. Physics and Chemistry of Minerals, 37, 1–9.
Gilmore, R.S. and Katz, J.L. (1982) Elastic properties of apatites. Journal of Materials Science, 17, 1131–1141.
Gross, K.A. and Berndt, C.C. (2002) Biomedical application of apatites. In M.J. Kohn, J. Rakovan, and J.M. Hughes, Eds., Phosphates: Geochemical, geobiological, and materials importance, 48, p. 631–672. Reviews in Mineralogy and Geochemistry, Mineralogical Society of America, Chantilly, Virginia.
Heinz, D.L. and Jeanloz, R. (1984) The equation of state of the gold calibration standard. Journal of Applied Physics, 55, 885–893.
Hughes, J.M. and Rakovan, J. (2002) The crystal structure of apatite, $Ca_5(PO_4)_3(F,OH,Cl)$. In M.J. Kohn, J. Rakovan, and J.M. Hughes, Eds., Phosphates: Geochemical, geobiological, and materials importance, 48, p. 1–12. Reviews in Mineralogy and Geochemistry, Mineralogical Society of America, Chantilly, Virginia.
Hughes, J.M., Cameron, M., and Crowley, K.D. (1989) Structural variations in natural F, OH, and Cl apatites. American Mineralogist, 74, 870–876.
Ivanova, T.I., Frank-Kamenetskaya, O.V., Kol'tsov, A.B., and Ugolkov, V.L. (2001) Crystal structure of calcium-deficient carbonated hydroxyapatite. Thermal decomposition. Journal of Solid State Chemistry, 160, 340–349.
Katz, J.L., Misra, A., Spencer, P., Wang, Y., Bumrerraj, S., Nomura, T., Eppell, S.J., and Tabib-Azar, M. (2007) Multiscale mechanics of hierarchical structure/property relationships in calcified tissues and tissue/material interfaces. Materials Science and Engineering A-Structural Materials, 27, 450–468.
Lang, J.R., Lueck, B., Mortensen, J.K., Russell, J.K., Stanley, C.R., and Thompson, J.F.H. (1995) Triassic-Jurassic silica-undersaturated and silica-saturated alkalic intrusions in the Cordillera of British Columbia: Implications for arc magmatism. Geology, 23, 451–454.
LeGeros, R.Z. (1965) Effects of carbonate on the lattice parameter of apatite. Nature, 206, 403–404.
——— (1991) Calcium phosphates in oral biology and medicine. Karger, New York.
LeGeros, R.Z., Trautz, O.R., Klein, E., and LeGeros, J.P. (1969) Two types of carbonate substitution in the apatite structure. Experimentia, 25, 5–7.
Leventouri, Th., Chakoumakos, B.C., Moghaddam, H.Y., and Perdikatsis, V. (2000) Powder neutron diffraction studies of a carbonate fluoapatite. Journal of Material Research, 15, 511–517.
Leventouri, Th., Chakoumakos, B.C., Papanearchou, N., and Perdikatsis, V. (2001) Comparison of crystal structure parameters of natural and synthetic apatites from neutron powder diffraction. Journal of Material Research, 16, 2600–2606.
Li, Y., Zheng, Y., Gong, B., and Fu, B. (2000) Carbon isotopes in eclogite and apatite separate from Huangzhen and Shima in SE Dabie. Science in China (Series D), 43, 449–457.
Liu, X., Shieh, S.R., Fleet, M.E., and Akhmetov, A. (2008) High-pressure study on lead fluorapatite. American Mineralogist, 93, 1581–1584.
Mao, H.K., Bell, P.M., Shaner, J.W., and Steinberg, D.J. (1978) Specific volume measurements of Cu, Mo, Pt, and Au and calibration of rub R1 fluorescence pressure gauge for 0.006 to 1 Mbar. Journal of Applied Physics, 49, 3276–3283.
Matsukage, K.N., Ono, S., Kawamoto, T., and Kikegawa, T. (2004) The compressibility of a natural apatite. Physical and Chemistry of Minerals, 31, 580–584.
McClellan, G.H. (1980) Mineralogy of carbonate fluorapatites. Journal of the Geological Society of London, 137, 675–681.
McClellan, G.H. and Lehr, J.R. (1969) Crystal chemical investigation of natural apatites. American Mineralogist, 54, 1374–1391.
Murayama, J.K., Nakai, S., Kato, M., and Kumazawa, M. (1986) A dense polymorph of $Ca_3(PO_4)_2$: A high pressure phase of apatite decomposition and its geochemical significance. Physics of the Earth and Planetary Interiors, 44, 293–303.
Nathan, Y. (1996) Mechanism for CO_3^{2-} substitution in carbonate-fluorapatite: Evidence from FTIR spectroscopy, ^{13}C NMR, and quantum mechanical calculations—Discussion. American Mineralogist, 81, 513–514.
Nelson, D.G.A. and Featherstone, J.D.B. (1982) Preparation, analysis, and characterization of carbonated apatites. Calcified Tissue International, 34, S69–S81.
Pan, Y. and Fleet, M.E. (2002) Compositions of the Apatite-group minerals: substitution mechanisms and controlling factors. In M.J. Kohn, J. Rakovan, and J.M. Hughes, Eds., Phosphates: Geochemical, geobiological, and materials importance, 48, p. 13–49. Reviews in Mineralogy and Geochemistry, Mineralogical Society of America, Chantilly, Virginia.
Regnier, P., Lasaga, A.C., Berner, R.A., Han, O.H., and Zilm, K.W. (1994) Mechanism for CO_3^{2-} substitution in carbonate-fluorapatite: Evidence from FTIR spectroscopy, ^{13}C NMR, and quantum mechanical calculations. American Mineralogist, 79, 809–818.
Rho, J.Y., Kuhn-Spearing, L., and Zioupos, P. (1998) Mechanical properties and the hierarchical structure of bone. Medical Engineering and Physics, 20, 92–102.
Santos, R.V. and Clayton, R.N. (1995) The carbonate content in high-temperature apatite: An analytical method applied to apatite from the Jacupiranga alkaline complex. American Mineralogist, 80, 336–344.
Snyders, R., Music, D., Sigumonrong, D., Schelnberger, B., Jensen, J., and Schneider, J.M. (2007) Experimental and ab initio study of the mechanical properties of hydroxyapatite. Applied Physics Letters, 90, 193902.
Trueman, N.A. (1966) Substitutions for phosphate ions in apatite. Nature, 210, 937–938.
Vignoles, M., Bonel, G., Holcomb, D.W., and Young, R.A. (1988) Influence of preparation conditions on the composition of type B carbonated hydroxyapatite and on the localization of the carbonate ions. Calcified Tissue International, 43, 33–40.
Walters, Jr., L.J., and Luth, W.C. (1969) Unit-cell dimensions, optical properties, halogen concentrations in several natural apatites. American Mineralogist, 54, 156–162.
Wilson, R.M., Elliott, J.C., and Dowker, S.E.P. (1999) Rietveld refinement of the crystallographic structure of human dental enamel apatites. American Mineralogist, 81, 1406–1414.
Wilson, R.M., Elliott, J.C., Dowker, S.E.P., and Smith, R.I. (2004) Rietveld structure refinement of precipitated carbonate apatite using neutron diffraction data. Biomaterials, 25, 2205–2213.
Zhai, S., Liu, X., Shieh, S.R., Zhang, L., and Ito, E. (2009) Equation of state of γ-tricalcium phosphate, γ-$Ca_3(PO_4)_2$, to lower mantle pressures. American Mineralogist, 94, 1388–1391.

MANUSCRIPT RECEIVED FEBRUARY 21, 2010
MANUSCRIPT ACCEPTED AUGUST 4, 2010
MANUSCRIPT HANDLED BY GUOYIN SHEN